

Time-Minimal Control of Dissipative Two-level Quantum Systems: the Generic Case

Bernard Bonnard,* Monique Chyba[†] and Dominique Sugny[‡]

October 22, 2018

Abstract

The objective of this article is to complete preliminary results from [4, 13] concerning the time-minimal control of dissipative two-level quantum systems whose dynamics is governed by Lindblad equations. The extremal system is described by a 3D-Hamiltonian depending upon three parameters. We combine geometric techniques with numerical simulations to deduce the optimal solutions.

Keywords. Time optimal control, conjugate and cut loci, quantum control

1 Introduction

In this article, we consider the time-minimal control analysis of two-level *dissipative* quantum systems whose dynamics is governed by *Lindblad equation*. More generally, according to [10], the dynamics of a finite-dimensional quantum system in contact with a dissipative environment is described by the evolution of the *density matrix* ρ given by the equation

$$i\frac{\partial\rho}{\partial t} = [H_0 + H_1, \rho] + i\mathcal{L}(\rho), \quad (1)$$

where H_0 is the field-free Hamiltonian of the system, H_1 represents the interaction with the control field and \mathcal{L} the dissipative part of the equation; $[A, B]$ is the commutator of the operators A and B defined by $[A, B] = AB - BA$. Equation (1) is written in units such that $\hbar = 1$. The components of the density matrix satisfy the following equations:

$$\begin{aligned} \dot{\rho}_{nn} &= -i[H_0 + H_1, \rho]_{nn} - \sum_{k \neq n} \gamma_{kn} \rho_{nn} + \sum_{k \neq n} \gamma_{nk} \rho_{kk} \\ \dot{\rho}_{kn} &= -i[H_0 + H_1, \rho]_{kn} - \Gamma_{kn} \rho_{kn}, \quad k \neq n \end{aligned} \quad (2)$$

*B. Bonnard is with the Institut de Mathématiques de Bourgogne, UMR CNRS 5584, 9 Avenue Alain Savary, BP 47 870 F-21078 DIJON Cedex FRANCE (bernard.bonnard@u-bourgogne.fr).

[†]M. Chyba is with the University of Hawaii, Department of Mathematics, Honolulu, HI 96822, USA (mchyba@math.hawaii.edu).

[‡]D. Sugny is with the Institut Carnot de Bourgogne, UMR 5209 CNRS-Université de Bourgogne, 9 Av. A. Savary, BP 47 870, F-21078 DIJON Cedex, FRANCE (dominique.sugny@u-bourgogne.fr).

where $1 \leq k \leq N$ and $1 \leq n \leq N$ for a N -level quantum system. The parameters γ_{kn} describe the population relaxation from state k to state n whereas Γ_{kn} is the dephasing rate of the transition from state k to state n . Note that not every positive parameter γ_{kn} or Γ_{kn} is acceptable from a physical point of view since the density matrix ρ must satisfy particular properties (trace conservation, hermitian operator and complete positivity [1, 9, 10]).

Particularizing now to the case $N = 2$, we assume that H_1 is of the form

$$H_1 = -\mu_x E_x - \mu_y E_y,$$

where the operators μ_x and μ_y are proportional to the Pauli matrices σ_x and σ_y in the eigenbasis of H_0 . The electric field is the superposition of two linearly polarized fields E_x and E_y and we assume that these two fields are in resonance with the Bohr frequency $E_2 - E_1$. In the *RWA approximation*, the time evolution of $\rho(t)$ satisfies the following form of the Lindblad equation

$$i \frac{\partial}{\partial t} \begin{pmatrix} \rho_{11} \\ \rho_{12} \\ \rho_{21} \\ \rho_{22} \end{pmatrix} = \begin{pmatrix} -i\gamma_{12} & -E^* & E & i\gamma_{21} \\ -E & -\omega - i\Gamma & 0 & E \\ E^* & 0 & \omega - i\Gamma & -E^* \\ i\gamma_{12} & E^* & -E & -i\gamma_{21} \end{pmatrix} \begin{pmatrix} \rho_{11} \\ \rho_{12} \\ \rho_{21} \\ \rho_{22} \end{pmatrix}, \quad (3)$$

where E is equal to $E = ue^{i\omega t}$ and u is the complex Rabi frequency of the laser field (the real and imaginary parts of u are the amplitudes of the real fields E_x and E_y up to a multiplicative constant). In Eq. (3), ω is the difference of energy between the ground and excited states of the system. In the interaction representation, Eq. (3) becomes

$$i \frac{\partial}{\partial t} \begin{pmatrix} \rho_{11} \\ \rho_{12} \\ \rho_{21} \\ \rho_{22} \end{pmatrix} = \begin{pmatrix} -i\gamma_{12} & -u^* & u & i\gamma_{21} \\ -u & -i\Gamma & 0 & u \\ u^* & 0 & -i\Gamma & -u^* \\ i\gamma_{12} & u^* & -u & -i\gamma_{21} \end{pmatrix} \begin{pmatrix} \rho_{11} \\ \rho_{12} \\ \rho_{21} \\ \rho_{22} \end{pmatrix}. \quad (4)$$

The interaction representation means that we have transformed the mixed-state ρ with the unitary transformation $U = \text{diag}(1, e^{i\omega t}, e^{-i\omega t}, 1)$. Since $\text{Tr}[\rho] = 1$, the density matrix ρ can be represented by the vector $q = {}^t(x, y, z)$ where $x = 2\Re[\rho_{12}]$, $y = 2\Im[\rho_{12}]$ and $z = \rho_{22} - \rho_{11}$ and q belongs to the Bloch ball $|q| \leq 1$. Equation (4) takes the form:

$$\begin{cases} \dot{x} = -\Gamma x + u_2 z \\ \dot{y} = -\Gamma y - u_1 z \\ \dot{z} = (\gamma_{12} - \gamma_{21}) - (\gamma_{12} + \gamma_{21})z + u_1 y - u_2 x \end{cases}. \quad (5)$$

$\Lambda = (\Gamma, \gamma_+, \gamma_-)$ is the set of parameters such that $\gamma_+ = \gamma_{12} + \gamma_{21}$ and $\gamma_- = \gamma_{12} - \gamma_{21}$ and they satisfy the following inequations $2\Gamma \geq \gamma_+ \geq |\gamma_-|$ derived from the Lindblad equation [12], the Bloch ball $|q| \leq 1$ being invariant. The control is $u = u_1 + iu_2$ where u_1 and u_2 are two real functions. We can write the control field $u = |u|e^{i\phi}$ where $|u| \leq M$ and up to a rescaling of the time and dissipative parameters we can assume that $|u| \leq 1$.

We consider the time-minimal transfer problem from a state q_0 to a state q_1 . Hence, we have to analyze a time-minimal control problem for a *bilinear system* of the form:

$$\dot{q} = F_0(q) + \sum_{i=1}^2 u_i F_i(q), \quad |u| \leq 1,$$

where the drift term F_0 depends upon three parameters. This problem is a very difficult problem whose analysis requires advanced mathematical tools from geometric control theory and numerical simulations.

Such analysis is motivated by physical reasons. It is a fundamental model in quantum control and more general problems can be handled by coupling such systems. Numerous optimal control results exist in the conservative case e.g. [6], but only partial ones for this problem: a pioneering work [13] assuming u real and a second one [4] for u complex but restricted to $\gamma_- = 0$.

The objective of this article is double. First of all, we introduce all the proper geometric tools to analyze the problem using Pontryagin maximum principle. Secondly, our aim is to make a complete study for every generic parameter in Λ , combining mathematical reasonings and numerical simulations based on *shooting techniques* and including computations of *conjugate points* to test optimality. Based on the Cotcot code [2], they can be used in practice to compute the true optimal control, once the physical parameters are identified.

The organization of this article is the following. In section 2, we complete the classification of the time-minimal synthesis of [13] corresponding to the case where u is real but introducing more general tools to handle the problem. It corresponds to a time-minimal control problem of a two-dimensional bilinear system in the single input case. The optimal synthesis for a fixed initial point can be constructed by gluing together local optimal syntheses. We can also make estimates of switching points by lifting the system on a semi-direct Lie group. *This classification is physically relevant to analyze the 3D-case because, using the symmetry of revolution of the problem, it gives the time-minimal synthesis for initial points $q_0 = {}^t(0, 0, \pm 1)$.* This geometric property is explained in section 3. Moreover, using spherical coordinates the system can be viewed as a system on a *two-sphere of revolution* coupled with the evolution of the distance to the origin, which represents the *purity* of the system. According to the maximum principle, smooth extremals are solutions of the Hamiltonian vector field \vec{H} where $H = H_0 + (H_1^2 + H_2^2)^{1/2}$, $H_i = \langle p, F_i(q) \rangle$, and the control components are given by $u_i = H_i / (H_1^2 + H_2^2)^{1/2}$, $i = 1, 2$. Non smooth extremals can be constructed by connecting smooth subarcs of the switching surface Σ : $H_1 = H_2 = 0$. A contribution of this article in section 3 is to classify the possible connections. We proved that every non smooth extremal is either a solution of the 2D-single input system, assuming u real, or occurs when meeting the equatorial plane of the Bloch ball. In the second case, the switching can be handled numerically using an integrator with an adaptative step. In the same section, we combine analytical and numerical analysis to determine the extremals and compute conjugate points. This completes the analysis from [4] in the integrable case. The physical interpretation is presented as a conclusion.

2 The 2D-case

Following [13], a first step in the analysis is to consider the following reduced system. Assuming u real, the x -coordinate is not controllable and we can consider the planar single-input system:

$$\begin{aligned} \dot{y} &= -\Gamma y - u_1 z \\ \dot{z} &= \gamma_- - \gamma_+ z + u_1 y, |u_1| \leq 1. \end{aligned}$$

It gives the time-optimal analysis of the control problem when the initial state $q(0) = (y(0), z(0))$ is a pure state on the z -axis, that is $q(0) = (0, \pm 1)$. We proceed as follows to make the analysis.

2.1 Symmetry group

A discrete symmetry group is associated to reflections with respect to the different axes. More precisely, if $w = -z$ then one gets the same system changing u_1 into $-u_1$ and γ_- into $-\gamma_-$. If $w = -y$ then one gets the same system changing u_1 into $-u_1$. In particular, concerning the time-minimal control problem, this amounts to exchange the trajectories σ_+ and σ_- corresponding respectively to $u_1 = 1$ and $u_1 = -1$. Also, according to this property, the time-minimal synthesis is symmetric with respect to the z -axis. This is connected to the symmetry of revolution of the whole system which is explained later.

2.2 The feedback classification

A preliminary step in our analysis is to consider the feedback classification problem [3]. The system is written in a more compact form as follows:

$$\dot{q} = F(q) + uG(q)$$

where F and G are affine vector fields. To make the feedback classification, we relax the control bound $|u| \leq 1$. The geometric invariants are related to the sets:

- $S = \{q, \det(G, [F, G]) = 0\}$ where are located the singular trajectories.
- $C = \{q, \det(F, G) = 0\}$ corresponding to the set of points where F and G are collinear.

They are obtained by straightforward computations of Lie brackets:

$$G = \begin{pmatrix} -z \\ y \end{pmatrix}, F = \begin{pmatrix} -\Gamma y \\ \gamma_- - \gamma_+ z \end{pmatrix}, [G, F] = \begin{pmatrix} (\gamma_+ - \Gamma)z - \gamma_- \\ (\gamma_+ - \Gamma)y \end{pmatrix}.$$

Hence, S is given by:

$$y[2(\Gamma - \gamma_+)z + \gamma_-] = 0$$

and if $\gamma_+ \neq \Gamma$, the singular set is defined by the two lines $y = 0$ and $z = \gamma_-/[2(\gamma_+ - \Gamma)]$. The collinear set is defined by:

$$\gamma_+ z^2 + \Gamma y^2 - \gamma_- z = 0$$

and is a closed curve formed by the union of two arcs of parabola, containing $(0, 0)$ and $(z_1, 0)$, with $z_1 = \gamma_-/\gamma_+$, which is the equilibrium state of the free motion. More generally, C contains the equilibrium points for the dynamics with constant control u_0 , since $F + u_0 G = 0$. In particular, the equilibrium point when $u_1 = 1$ is given by

$$C_1 : y = \frac{\gamma_-}{1 + \gamma_+ \Gamma}, z = -\Gamma y.$$

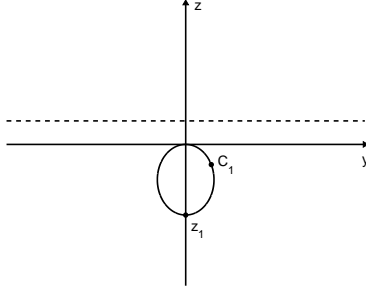


Figure 1: Diagram of the sets S and C in solid lines for $\gamma_- = -0.2$, $\gamma_+ = 0.4$ and $\Gamma = 1$. The equation of the horizontal dashed line is $z = \gamma_-/2(\gamma_+ - \Gamma)$.

The collinear set C shrinks into a point when $\gamma_- = 0$. Computing the intersection of C with the singular line $z = \gamma_-/[2(\gamma_+ - \Gamma)]$, one gets:

$$\Gamma y^2 = \frac{\gamma_-^2}{4(\gamma_+ - \Gamma)^2}(\gamma_+ - 2\Gamma).$$

If $\gamma_- \neq 0$, since $2\Gamma \geq \gamma_+$, one deduces that the intersection is empty except in the case where $\gamma_+ = 2\Gamma$. An important consequence is to simplify the classification of the optimal syntheses. We represent on Fig. 1 the sets S and C for a situation with $\gamma_- < 0$ and $\gamma_+ - \Gamma < 0$. Another feedback invariant is the optimality status of singular trajectories. Using the generalized Legendre-Clebsch condition, it is splitted into fast and slow directions. In the 2D-case, it is tested by Lie brackets configurations and can be computed by introducing:

$$D = \det(G, [[G, F], G]), \quad D'' = \det(G, F).$$

The trajectory is time-optimal in the so-called hyperbolic case $DD'' > 0$ and time-maximal in the so-called elliptic case $DD'' < 0$. Computing Lie brackets of length 3, we have:

$$[[G, F], G] = \begin{pmatrix} 2(\gamma_+ - \Gamma)y \\ \gamma_- - 2(\gamma_+ - \Gamma)z \end{pmatrix}$$

and

$$[[G, F], F] = \begin{pmatrix} (\gamma_+ - \Gamma)(\gamma_- - \gamma_+ z) + \Gamma[(\gamma_+ - \Gamma)z - \gamma_-] \\ (\gamma_+ - \Gamma)^2 y \end{pmatrix}.$$

Hence:

$$D'' = \begin{vmatrix} -z & -\Gamma y \\ y & \gamma_- - \gamma_+ z \end{vmatrix}, \quad D = \begin{vmatrix} -z & 2(\gamma_+ - \Gamma)y \\ y & \gamma_- - 2(\gamma_+ - \Gamma)z \end{vmatrix}.$$

For the singular direction $y = 0$, we get:

$$DD'' = 2z^2(\gamma_+ - \Gamma)\gamma_+(z - \frac{\gamma_-}{2(\gamma_+ - \Gamma)})(z - \frac{\gamma_-}{\gamma_+}).$$

Near the origin, the sign is always positive if $\gamma_- \neq 0$. If $\gamma_- = 0$, the sign is given by $(\gamma_+ - \Gamma)$. For the singular direction $z = \gamma_-/[2(\gamma_+ - \Gamma)]$, we have:

$$DD'' = \frac{y^2}{2(\gamma_+ - \Gamma)}[\gamma_-^2(\gamma_+ - 2\Gamma) - 4\Gamma y^2(\gamma_+ - \Gamma)^2].$$

Hence, near the origin, the optimality is given by the sign of $(\gamma_+ - 2\Gamma)(\gamma_+ - \Gamma)$. Moreover, since $\Gamma \geq \gamma_+/2$, one gets that $DD'' > 0$ if $\gamma_+ - \Gamma < 0$ and $DD'' < 0$ if $\gamma_+ - \Gamma > 0$.

2.3 Computation of a normal form

In order to analyze the time-optimal control, we compute a global normal form up to a polar singularity for the action of the feedback group. A first step is to linearize the vector field G since it is connected to the evaluation of the switching times. One further normalization is to straight the horizontal singular line: $z = \gamma_-/[2(\gamma_+ - \Gamma)]$. Using polar coordinates:

$$y = \rho \cos \phi, \quad z = \rho \sin \phi,$$

one gets:

$$\begin{aligned} \dot{\rho} &= \gamma_- \sin \phi + \rho[-\Gamma + (\Gamma - \gamma_+) \sin^2 \phi] \\ \dot{\phi} &= \frac{\gamma_- \cos \phi}{\rho} + (\Gamma - \gamma_+) \frac{\sin(2\phi)}{2} + u_1. \end{aligned}$$

If we use the coordinates $x = \rho^2/2$ and z , the system becomes:

$$\begin{aligned} \dot{x} &= -2\Gamma x + \gamma_- z + z^2(\Gamma - \gamma_+) \\ \dot{z} &= \gamma_- - \gamma_+ z + u_1 \sqrt{2x - z^2}. \end{aligned}$$

Making a feedback transformation of the form $u_1 \rightarrow \beta u_1$ where β is a function of x and z , we can consider the system:

$$\begin{aligned} \dot{x} &= -2\Gamma x + \gamma_- z + z^2(\Gamma - \gamma_+) \\ \dot{z} &= \gamma_- - \gamma_+ z + u_1. \end{aligned}$$

If we set $z = Z + z_0$ where $z_0 = \gamma_-/[2(\gamma_+ - \Gamma)]$, we obtain the system:

$$\begin{aligned} \dot{x} &= \frac{\gamma_-^2}{4(\gamma_+ - \Gamma)} - 2\Gamma x + (\Gamma - \gamma_+)z^2 \\ \dot{z} &= \frac{\gamma_- (\gamma_+ - 2\Gamma)}{2(\gamma_+ - \Gamma)} - \gamma_+ z + u_1. \end{aligned}$$

In this simplified model where the control is rescaled by the positive parameter β , we keep most of the information about the initial system. In particular, all the feedback invariants are preserved: the collinear set corresponds to $\dot{x} = 0$ and the singular set is identified to $z = 0$ with its optimality status, while we have wiped out the singular line $y = 0$. Due to the feedback transformation, we lose however the singularities of the vector fields $F + G$ and $F - G$ and also the saturation phenomenon of the singular control.

For the simplified model, the adjoint system takes the form:

$$\begin{aligned} \dot{p}_x &= 2\Gamma p_x \\ \dot{p}_z &= -2z p_x (\Gamma - \gamma_+) + p_z \gamma_-, \end{aligned}$$

and can be easily integrated to compute the time-minimal synthesis.

2.4 The saturation phenomenon

One interesting property which is not captured by the normal form is when the singular control is saturating along the horizontal singular line $z = \gamma_- / [2(\gamma_+ - \Gamma)]$. Introducing $D' = \det(G, [[G, F], F])$, we get on the singular line: $D' = y\gamma_-(2\Gamma - \gamma_+)$. The singular control is given by:

$$u_s = -\frac{D'}{D} = \frac{\gamma_-(\gamma_+ - 2\Gamma)}{2y(\Gamma - \gamma_+)},$$

and saturation occurs when $|u_s| = 1$. Observe that if $\gamma_-(2\Gamma - \gamma_+) \neq 0$ then the singular control is never admissible when $y = 0$.

2.5 The switching function

For the true system, the switching function is more intricate but can be still analyzed using geometric and numerical techniques. The switching function Φ is given by $\Phi(t) = p(t)G(q(t))$ and switching occurs when $\Phi(t) = 0$. By construction, G is tangent to the circle S^1 , hence is rotating when we follow an arc curve σ_+ or σ_- . The dynamics of p is given by the adjoint equation:

$$\dot{p} = -p\left(\frac{\partial F}{\partial q} + u\frac{\partial G}{\partial q}\right), \quad u = \pm 1.$$

The corresponding dynamics is linear and p can be either oscillating if the eigenvalues are complex or non oscillating if they are real.

An equivalent but more geometric test is the use of the standard θ -function introduced in [7] and defined as follows. Let v be the tangent vector solution of the variational equation:

$$\dot{v} = \left(\frac{\partial F}{\partial q} + u\frac{\partial G}{\partial q}\right)v, \quad u = \pm 1,$$

whose dynamics is similar to the one of the adjoint vector. Let $t_1 < t_2$ be two consecutive switching times on an arc σ_+ or σ_- . One can set $t_1 = 0$ and $t_2 = t$. By definition, we have:

$$p(0)G(q(0)) = p(t)G(q(t)) = 0.$$

We denote by $v(\cdot)$ the solution of the variational equation such that $v(t) = G(q(t))$ and where this equation is integrated backwards from time t to time 0. By construction $p(0)v(0) = 0$ and we deduce that at time 0, $p(0)$ is orthogonal to $G(q(0))$ and to $v(0)$. Therefore, $v(0)$ and $G(q(0))$ are collinear; $\theta(t)$ is defined as the angle between $G(q(0))$ and $v(0)$ measured counterclockwise. One deduces that switching occurs when $\theta(t) = 0$ [π]. In the analytic case, $\theta(t)$ can be computed using Lie brackets. Indeed, for $u = \varepsilon$, $\varepsilon = \pm 1$, we have by definition

$$v(0) = e^{-t\text{ad}(F+\varepsilon G)}G(q(t)),$$

and in the analytic case, the ad-formulae gives :

$$v(0) = \sum_{n \geq 0} \frac{(-t)^n}{n!} \text{ad}^n(F + \varepsilon G)G(q(t)).$$

Here, to make the computation explicit, we take advantage of the fact that we can lift our bilinear system into an invariant system onto the semi-direct Lie group $GL(2, \mathbb{R}) \times_S \mathbb{R}^2$ identified to the set of matrices of $GL(3, \mathbb{R})$:

$$\begin{pmatrix} 1 & 0 \\ g & v \end{pmatrix}, g \in GL(2, \mathbb{R}), v \in \mathbb{R}^2,$$

acting on the subspace of vectors in \mathbb{R}^3 : $\begin{pmatrix} 1 \\ q \end{pmatrix}$.

Lie brackets computations are defined as follows. We set:

$$F(q) = Aq + a, G(q) = Bq,$$

and F, G are identified to $(A, a), (B, 0)$ in the Lie algebra $\underline{gl}(2, \mathbb{R}) \times \mathbb{R}^2$. The Lie brackets computations on the semi-direct product are defined by:

$$[(A', a'), (B', b')] = ([A', B'], A'b' - B'a').$$

We now compute $\exp[-tad(F + \varepsilon G)]$. The first step consists in determining $\exp[-tad(A + \varepsilon B)]$ which amounts to compute $ad(A + \varepsilon B)$. We write $\underline{gl}(2, \mathbb{R}) = c \oplus \underline{sl}(2, \mathbb{R})$ where c is the center

$$\mathbb{R} \begin{pmatrix} 1 & 0 \\ 0 & 1 \end{pmatrix}.$$

We choose the following basis of $\underline{sl}(2, \mathbb{R})$:

$$B = \begin{pmatrix} 0 & -1 \\ 1 & 0 \end{pmatrix}, C = \begin{pmatrix} 0 & 1 \\ 1 & 0 \end{pmatrix} \text{ and } D = \begin{pmatrix} 1 & 0 \\ 0 & -1 \end{pmatrix}.$$

The matrix A is decomposed into:

$$A = \begin{pmatrix} -\Gamma & 0 \\ 0 & -\gamma_+ \end{pmatrix} = \begin{pmatrix} \lambda & 0 \\ 0 & \lambda \end{pmatrix} + \begin{pmatrix} s & 0 \\ 0 & -s \end{pmatrix}$$

and hence $\lambda = -(\Gamma + \gamma_+)/2$ and $s = (\gamma_+ - \Gamma)/2$. In the basis (B, C, D) , $ad(A + \varepsilon B)$ is represented by the matrix:

$$\begin{pmatrix} 0 & -2s & 0 \\ -2s & 0 & 2\varepsilon \\ 0 & -2\varepsilon & 0 \end{pmatrix}.$$

The characteristic polynomial is $P(\lambda) = -\lambda(\lambda^2 + 4(\varepsilon^2 - s^2))$ and the eigenvalues are $\lambda = 0$ and $\lambda_i = \pm 2\sqrt{s^2 - \varepsilon^2}$, $i = 1, 2$; λ_1 and λ_2 are distinct and real if $|\gamma_+ - \Gamma| > 2$ and we note $\lambda_1 = 2\sqrt{\varepsilon^2 - s^2}$, $\lambda_2 = -\lambda_1$; λ_1 and λ_2 are distinct and imaginary if $|\gamma_+ - \Gamma| < 2$ and we note $\lambda_1 = 2i\sqrt{\varepsilon^2 - s^2}$, $\lambda_2 = -\lambda_1$. To compute $e^{-tad(A + \varepsilon B)}$, we must distinct two cases.

Real case: In the basis B, C, D , the eigenvectors corresponding to $\{0, \lambda_1, \lambda_2\}$ are respectively: $v_0 = {}^t(\varepsilon, 0, s)$, $v_1 = {}^t(2s, -\lambda_1, 2\varepsilon)$ and $v_2 = {}^t(2s, -\lambda_2, 2\varepsilon)$. Therefore, in this eigenvector basis, $\exp[-tad(A + \varepsilon B)]$ is the diagonal matrix: $\text{diag}(1, e^{-\lambda_1 t}, e^{-\lambda_2 t})$. To compute $\exp[-tad(A + \varepsilon B)]B$, we use the decomposition

$$B = \alpha v_0 + \beta v_1 + \gamma v_2,$$

with:

$$\alpha = \frac{\varepsilon}{\varepsilon^2 - s^2}, \quad \beta = \frac{-\lambda_2 s}{2(\lambda_2 - \lambda_1)(\varepsilon^2 - s^2)}, \quad \gamma = \frac{-\lambda_1 s}{2(\lambda_1 - \lambda_2)(\varepsilon^2 - s^2)}.$$

Hence one gets:

$$e^{-t\text{ad}(A+\varepsilon B)}B = \alpha v_0 + \beta e^{-\lambda_1 t}v_1 + \gamma e^{-\lambda_2 t}v_2.$$

To test the collinearity at q_0 , we compute

$$\det(B(q_0), e^{-t\text{ad}(A+\varepsilon B)}B(q_0)) = 0$$

where the determinant is equal to

$$(z_0^2 - y_0^2)(\alpha s + 2\varepsilon(\beta e^{-\lambda_1 t} + \gamma e^{-\lambda_2 t})) + 2y_0 z_0(\lambda_1 \beta e^{-\lambda_1 t} + \lambda_2 \gamma e^{-\lambda_2 t}).$$

Using the fact that this last expression has at most two zeros, one being for $t = 0$, it is straightforward to check that for $q_0 = {}^t(0, 1)$, this expression only vanishes at $t = 0$. This proves the result numerically checked in [13] that there is *at most one switching*. This analysis can be generalized to any initial condition.

Imaginary case: In this case, we note $\lambda_1 = i\theta$ the eigenvalue associated to the eigenvector ${}^t(2s, -i\theta, 2\varepsilon)$. We consider the real part $v_1 = {}^t(2s, 0, 2\varepsilon)$ and the imaginary part $v_2 = {}^t(0, -\theta, 0)$. In the basis $v_0 = {}^t(\varepsilon, 0, s)$, v_1 , v_2 , $\text{ad}(A + \varepsilon B)$ takes the normal form:

$$\text{diag}\left(0, \begin{pmatrix} 0 & \theta \\ -\theta & 0 \end{pmatrix}\right).$$

Hence, we have in this basis:

$$e^{-t\text{ad}(A+\varepsilon B)} = \text{diag}\left(1, \begin{pmatrix} \cos(\theta t) & -\sin(\theta t) \\ \sin(\theta t) & \cos(\theta t) \end{pmatrix}\right).$$

We decompose B in the same basis:

$$B = \alpha v_0 + \beta v_1 + \gamma v_2,$$

where

$$\alpha = \frac{\varepsilon}{\varepsilon^2 - s^2}, \quad \beta = -\frac{s}{2(\varepsilon^2 - s^2)}, \quad \gamma = 0.$$

Hence, we get:

$$e^{-t\text{ad}(A+\varepsilon B)}B = \alpha v_0 + \beta[\cos(\theta t)v_1 + \sin(\theta t)v_2].$$

Computing we obtain:

$$\det(Bq_0, e^{-t\text{ad}(A+\varepsilon B)}B(q_0)) = (z_0^2 - y_0^2)(\alpha s + 2\varepsilon\beta \cos(\theta t)) + 2\beta\theta \sin(\theta t)y_0 z_0$$

which vanishes for two values of t in $[0, 2\pi/\theta[$ if $y_0 \neq z_0$. These two values coincide for $q_0 = {}^t(0, 1)$. Hence *the switchings occur periodically with a period of $2\pi/\theta$* which confirms the numerical simulations of [13].

Case $\gamma_- \neq 0$: The Lie bracket is given by:

$$[(A', a'), (B', b')] = ([A', B'], A'b' - B'a').$$

We note (e_1, e_2) the \mathbb{R}^2 -canonical basis and $a = \gamma_- e_2$. We have:

$$\begin{aligned} \text{ad}(A + \varepsilon B, a) \cdot (B, 0) &= ([A + \varepsilon B, B], -Ba) \\ &= ([A, B], -Ba), \end{aligned}$$

$$\begin{aligned} \text{ad}^2(A + \varepsilon B, a) \cdot (B, 0) &= [(A + \varepsilon B, a), ([A, B], -Ba)] \\ &= (\text{ad}^2(A + \varepsilon B, B), -(A + \varepsilon B)Ba - [A, B]a). \end{aligned}$$

More generally, one gets:

$$\text{ad}^k(A + \varepsilon B, a) \cdot (B, 0) = (\text{ad}^k(A + \varepsilon B) \cdot B, v_k)$$

where v_k is given by the recurrence relation:

$$v_k = -\text{ad}^{k-1}(A + \varepsilon B) \cdot Ba + (A + \varepsilon B)v_{k-1}.$$

The computation is intricate but simplifies if $\gamma_+ = \Gamma$ since in this case $\text{ad}^k(A + \varepsilon B) \cdot B = 0$ for $k \geq 1$. Numerical simulations have to be used to compute the switchings sequence.

Generalization: This technique can be generalized to the time-minimal control problem in the full control case, replacing the control domain $|u| \leq 1$ by $|u_1|, |u_2| \leq 1$.

2.6 The time-minimal synthesis

We use [3] as general reference on time-minimal synthesis, see also [7]. The initial condition is fixed to $q_0 = {}^t(0, 1)$ and we consider the problem of constructing the time-minimal synthesis from this initial point. This amounts to compute two objects:

- The switching locus $\Sigma(q_0)$ of optimal trajectories which is deduced from the switching locus of extremal trajectories.
- The cut locus $C(q_0)$ which is formed by the set of points where a minimizer ceases to be optimal.

In order to achieve this task, we must glue together local time minimal syntheses which are classified. To be more precise, we recover the case (d) of [13], the gluing being indicated on Fig. 2 on which we have represented the local extremal classifications of [3] which are crucial to deduce the optimal syntheses. In this case, the cut locus is a segment of the z -axis and its birth is located at the initial point $(0, 1)$ which is a consequence of the elliptic situation. The switching locus is the union of a fast singular trajectory, corresponding to an hyperbolic point and a curve $\Sigma_1(q_0)$ corresponding to parabolic points (for the terminology see [3]). Note also the importance of the tangential point where arcs σ_+ and σ_- are tangent leading to the fish-shaped accessibility set $A^+(q_0)$ represented on Fig. 3. This set is not closed since the arc σ^1 starting from $(0, z_1)$ is not in $A^+(q_0)$. We next list the micro-local situations we need to construct the synthesis.

- **Ordinary switching points:** The local synthesis is given by $\sigma_- \sigma_+$ or $\sigma_+ \sigma_-$. The two cases are distinguished using for instance the clock form $\omega = pdq$ with $\langle p, G \rangle = 0$ and $\langle p, F \rangle = 1$ which is also useful to get more global results.

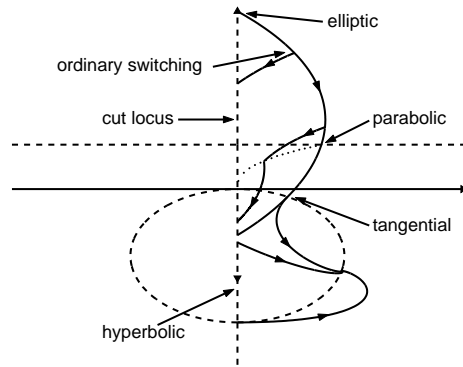


Figure 2: Cut and switching loci for the case $\gamma_- < 0$. The sets C and S are represented in dashed lines, the switching locus in dotted lines.

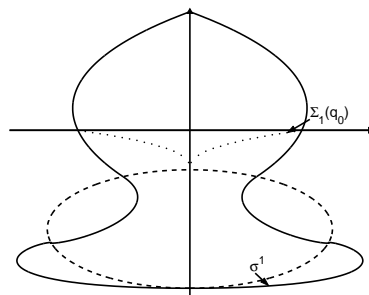


Figure 3: Poisson shape of the accessibility set.

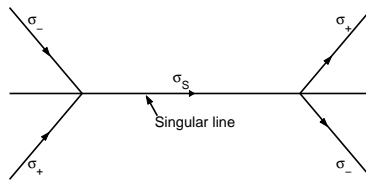


Figure 4: Structure of the extremals for the hyperbolic case.

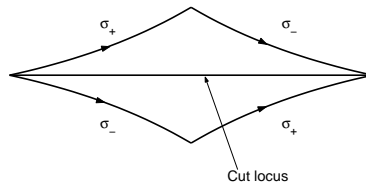


Figure 5: Elliptic case.

- **Hyperbolic case:** Existence of a fast singular admissible trajectory. The optimal synthesis is of the form $\sigma_{\pm}\sigma_s\sigma_{\pm}$ where σ_s is a singular arc (see Fig. 4).
- **Elliptic case:** Existence of a slow admissible singular trajectory. An optimal arc is bang-bang with at most one switching. Not every extremal trajectory is optimal and we have birth of a cut locus (see Fig. 5).
- **Parabolic point:** It corresponds to a non-admissible singular direction. Every extremal curve is bang-bang with at most two switchings. In our case, the initial point is fixed and the switching locus starts with the intersection of σ_- with the singular line (see Fig. 6).
- **Saturating case:**
A *fast* singular trajectory is saturating at a point M : birth of a switching curve at M (see Fig. 7).
- **A $C \cap S \neq \emptyset$ case:**
A *fast* singular trajectory meets the set C and becomes *slow*.

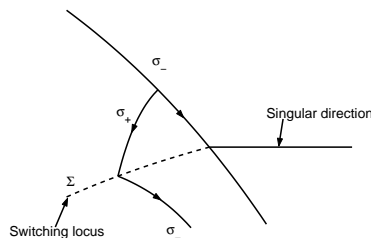


Figure 6: Parabolic case.

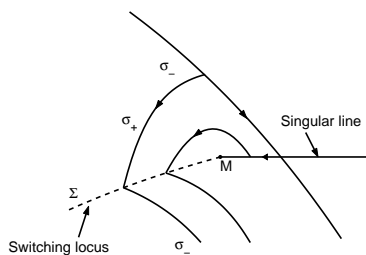


Figure 7: Saturating case

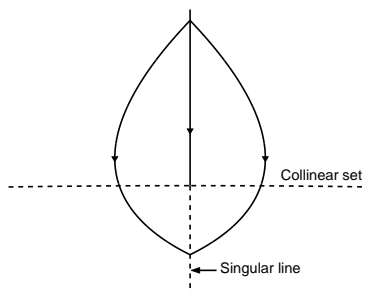


Figure 8: A $C \cap S \neq \emptyset$ case

2.7 Classification of the optimal syntheses

We describe the different time-optimal syntheses in the single-input case. Without loss of generality, we restrict the study to the initial point $q_0 = {}^t(0, 1)$. The classification is done with respect to the relative positions of the feedback invariants C and S and to the optimal status of singular extremals which are fast or slow according to the values of Γ , γ_+ and γ_- .

For $\gamma_- = 0$, the set C is restricted to the origin and we have two cases according to the sign of $\Gamma - \gamma_+$. Note that the form of the extremals σ_+ and σ_- starting from q_0 depends on the sign of $|\Gamma - \gamma_+| - 2$. Two cases for $\Gamma > \gamma_+$ are presented in [13]. We complete this study with the optimal synthesis for $\Gamma < \gamma_+$ and $|\Gamma - \gamma_+| < 2$ displayed in Fig. 9a.

For $\gamma_- \neq 0$, we distinguish four cases according to the signs of γ_- and $\Gamma - \gamma_+$. One case ($\Gamma > \gamma_+$ and $\gamma_- < 0$) is treated in [13]. We consider here three types of optimal synthesis represented in Fig. 9b, 9c and 9d. Note that in a same class of synthesis the reachable set from the initial point q_0 depends on the dissipative parameters which can modify the structure of the synthesis. The last case $\gamma_- > 0$ and $\gamma_+ > \Gamma$ can be deduced from the case $\gamma_- > 0$ and $\gamma_+ < \Gamma$ since the horizontal singular line plays no role in both cases. The synthesis of Fig. 9d is very similar to the one of Fig. 2 except the fact that a part of the horizontal singular line is admissible. The switching locus has been computed numerically using the switching function Φ .

The role of the parameter γ_- is clearly illustrated in Figs. 9a and 9c. The case $\gamma_- = 0$ is a degenerate case where the set C shrinks into a point. The variation of γ_- induces a *bifurcation* of the control system leading to new structures of the optimal synthesis. For $\gamma_- \neq 0$, the set C is the union of two branches

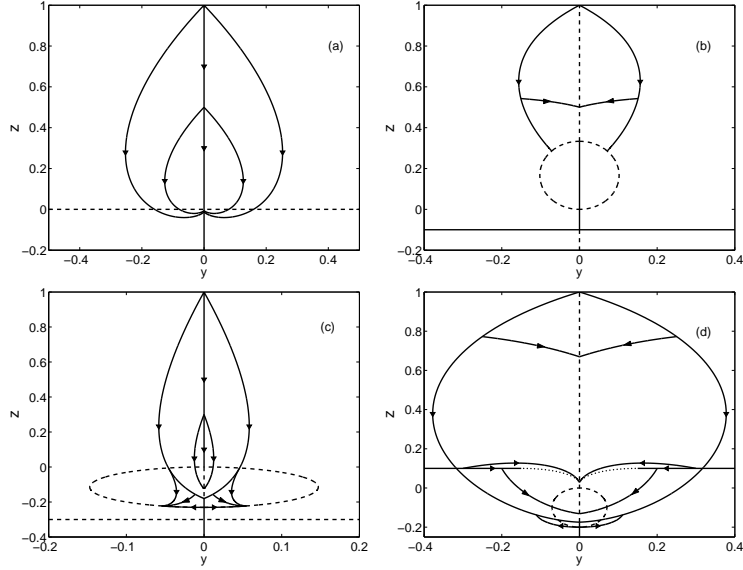


Figure 9: Optimal syntheses for (a) ($\Gamma = 1.1$, $\gamma_+ = 1.6$, $\gamma_- = 0$), (b) ($\Gamma = 4$, $\gamma_+ = 1.5$, $\gamma_- = 0.5$), (c) ($\Gamma = 4$, $\gamma_+ = 6.5$, $\gamma_- = -1.5$) and (d) ($\Gamma = 1$, $\gamma_+ = 0.5$, $\gamma_- = -0.1$). Solid and dashed vertical and horizontal lines correspond respectively to fast and slow singular lines. The set C is represented in dashed lines. The switching locus is plotted in dotted line. In (d), only the admissible singular horizontal line is represented in solid line.

of parabola. The optimal status of the vertical singular line changes when this line crosses the set C in Fig. 9c.

3 The bi-input case

3.1 Geometric analysis

The system is written in short in Cartesian coordinates as follows:

$$\dot{q} = F_0(q) + u_1 F_1(q) + u_2 F_2(q), \quad |u| \leq 1.$$

Introducing the Hamiltonians $H_i = \langle p, F_i \rangle$, $i = 0, 1, 2$, the pseudo-Hamiltonian associated to the time-optimal control problem is:

$$H = H_0 + \sum_{i=1}^2 u_i H_i + p_0,$$

where $p_0 \leq 0$. The time-optimal control is given outside the switching surface Σ : $H_1 = H_2 = 0$, by $u_i = H_i / \sqrt{H_1^2 + H_2^2}$, $i = 1, 2$, with the corresponding true Hamiltonian:

$$H_r = H_0 + \sqrt{H_1^2 + H_2^2},$$

whose solutions (outside Σ) are smooth and are called *extremals of order 0*. More general non smooth extremals can be obtained by connecting such arcs through Σ .

To make the geometric analysis and to highlight the symmetry of revolution, the system is written using the spherical coordinates:

$$x = \rho \sin \phi \cos \theta, \quad y = \rho \sin \phi \sin \theta, \quad z = \rho \cos \phi$$

and a feedback transformation:

$$v_1 = u_1 \cos \theta + u_2 \sin \theta, \quad v_2 = -u_1 \sin \theta + u_2 \cos \theta.$$

We obtain the system:

$$\dot{\rho} = \gamma_- \cos \phi - \rho(\gamma_+ \cos^2 \phi + \Gamma \sin^2 \phi) \quad (6a)$$

$$\dot{\phi} = -\frac{\gamma_- \sin \phi}{\rho} + \frac{\sin(2\phi)}{2}(\gamma_+ - \Gamma) + v_2 \quad (6b)$$

$$\dot{\theta} = -\cot \phi v_1. \quad (6c)$$

Hence, one deduces that the true Hamiltonian is:

$$H_r = [\gamma_- \cos \phi - \rho(\gamma_+ \cos^2 \phi + \Gamma \sin^2 \phi)]p_\rho + p_\phi \left[-\frac{\gamma_- \sin \phi}{\rho} + \frac{\sin(2\phi)}{2}(\gamma_+ - \Gamma) \right] + \sqrt{p_\phi^2 + p_\theta^2 \cot^2 \phi}.$$

From this, we deduce the following lemma:

Lemma 1. (i)- *The angle θ is a cyclic variable and p_θ is a first integral (symmetry of revolution).*

(ii)- *For $\gamma_- = 0$, using the coordinate $r = \ln \rho$, the Hamiltonian takes the form:*

$$H_r = -(\gamma_+ \cos^2 \phi + \Gamma \sin^2 \phi)p_r + \sin(2\phi)(\gamma_+ - \Gamma)p_\phi + \sqrt{p_\phi^2 + p_\theta^2 \cot^2 \phi}. \quad (7)$$

Hence, r is an additional cyclic variable and p_r is a first integral. The system is thus Liouville integrable.

As a consequence, we can deduce two properties. First of all, the z -axis is an axis of revolution and the state $q_0 = {}^t(0, 0, 1)$ is a pole. This means that by making a rotation around (Oz) of the extremal synthesis for the 2D-system, we generate the extremal synthesis for the 3D-system.

More generally, we have for $\gamma_- = 0$ a system on the *two-sphere of revolution* described by Eqs. (6b) and (6c) coupled with the one dimensional system (6a) describing the evolution of the physical variable ρ corresponding to the purity of the system. Moreover, the system is invariant for the transformation $\phi \mapsto \pi - \phi$ which is associated to a reflexional symmetry with respect to the equator for the system (6) restricted to the two-sphere of revolution. This property is crucial in the analysis of the integrable case.

If $\gamma_- \neq 0$ then the situation is more intricate. The extremals solutions of order 0 satisfy the equations which are singular for $\rho = 0$:

$$\begin{aligned} \dot{\rho} &= \gamma_- \cos \phi - \rho(\gamma_+ \cos^2 \phi + \Gamma \sin^2 \phi) \\ \dot{\phi} &= -\frac{\gamma_- \sin \phi}{\rho} + \frac{\sin(2\phi)}{2}(\gamma_+ - \Gamma) + \frac{p_\phi}{Q} \\ \dot{\theta} &= \frac{p_\theta \cot^2 \phi}{Q}, \end{aligned} \quad (8)$$

and

$$\begin{aligned}\dot{p}_\rho &= (\gamma_+ \cos^2 \phi + \Gamma \sin^2 \phi)p_\rho - \frac{\gamma_- \sin \phi}{\rho^2} p_\phi \\ \dot{p}_\phi &= [\gamma_- \sin \phi + \rho(\Gamma - \gamma_+) \sin(2\phi)]p_\rho - \left[-\frac{1}{\rho} \cos \phi \gamma_- + (\gamma_+ - \Gamma) \cos(2\phi)\right]p_\phi + \frac{p_\theta^2 \cos \phi}{Q \sin^3 \phi} \\ \dot{p}_\theta &= 0,\end{aligned}$$

$$\text{where } Q = \sqrt{p_\theta^2 \cot^2 \phi + p_\phi^2}.$$

3.2 Regularity analysis

The smooth extremal curves solutions of \vec{H}_r are not the only extremals because more complicated behaviors are due to the existence of the switching surface Σ : $H_1 = H_2 = 0$. Hence, in order to get singularity results, we must analyze the possible connections of two smooth extremals crossing Σ to generate a piecewise smooth extremal. This can also generate complex singularities of the Fuller type, where the switching times accumulate. In our problem, the situation is less complex because of the symmetry of revolution. The aim of this section is to make the singularity analysis of the extremals near Σ .

The structure of optimal trajectories is described by the following proposition.

Proposition 1. *Every optimal trajectory is:*

- *Either an extremal trajectory with $p_\theta = 0$ contained in a meridian plane and time-optimal solution of the 2D-system, where $u = (u_1, 0)$.*
- *Or subarcs solutions of \vec{H}_r , where $p_\theta \neq 0$ with possible connections in the equator plane for which $\phi = \pi/2$.*

Proof. The first assertion is clear. If $p_\theta = 0$ then extremals are such that $\dot{\theta} = 0$ and up to a rotation around the z -axis, they correspond to solutions of the 2D-system. The switching surface Σ is defined by: $p_\theta \cot \phi = p_\phi = 0$. We cannot connect an extremal with $p_\theta \neq 0$ to an extremal where $p_\theta = 0$ since at the connection the adjoint vector has to be continuous. Hence, the only remaining possibility is to connect subarcs of \vec{H}_r with $p_\theta \neq 0$ at a point of Σ leading to the conditions $p_\phi = 0$ and $\phi = \pi/2$. \square

Further work is necessary to analyze the behaviors of such extremals near Σ .

Normal form: A first step in the analysis is to construct a normal form. Taking the system in spherical coordinates and setting $\psi = \pi/2 - \phi$, the approximation is:

$$\begin{aligned}\dot{\rho} &= \gamma_- \psi - \rho[\Gamma + (\gamma_+ - \Gamma)\psi^2] \\ \dot{\psi} &= \frac{\gamma_-}{\rho}(1 - \psi^2/2) - \psi(\gamma_+ - \Gamma) - v_2 \\ \dot{\theta} &= -\psi v_1,\end{aligned}$$

with the corresponding Hamiltonian:

$$H_r = p_\rho[\gamma_- \psi - \rho(\Gamma + (\gamma_+ - \Gamma)\psi^2)] + p_\psi\left[\frac{\gamma_-}{\rho}(1 - \psi^2/2) - \psi(\gamma_+ - \Gamma)\right] + \sqrt{p_\psi^2 + p_\theta^2 \psi^2}. \quad (9)$$

Proposition 2. *Near $\psi = 0$, $p_\psi = 0$, we have two distinct cases for optimal trajectories:*

- *If $\gamma_- = 0$, for the 2D-system, the line $\psi = 0$ is a singular trajectory with admissible zero control if $\gamma_+ - \Gamma \neq 0$. It is slow if $(\gamma_+ - \Gamma) > 0$ and fast if $(\gamma_+ - \Gamma) < 0$. Hence, for this system, we get only extremal trajectories through Σ in the case $(\gamma_+ - \Gamma) < 0$, where ψ is of order t and p_ψ of order t^2 . They are the only non-smooth optimal trajectories passing through Σ .*
- *If $\gamma_- \neq 0$, for the 2D-system, the set $\psi = p_\psi = 0$ becomes a set of ordinary switching points where ψ and p_ψ are of order t . Moreover, connections for extremals of \vec{H}_r are eventually possible, depending upon the set of parameters and initial conditions.*

Proof. For the normal form, the adjoint system is:

$$\begin{aligned} \dot{p}_\rho &= p_\rho(\Gamma + (\gamma_+ - \Gamma)\psi^2) + \frac{p_\psi}{\rho^2}\gamma_-(1 - \frac{\psi^2}{2}) \\ \dot{p}_\psi &= -p_\rho(\gamma_- - 2\psi\rho(\gamma_+ - \Gamma)) + p_\psi\left(\frac{\gamma_- \psi}{\rho} + (\gamma_+ - \Gamma)\right) + v_1 p_\theta. \end{aligned} \quad (10)$$

In order to make the evaluation of smooth arcs reaching or departing from Σ , the technique is simple: a solution of the form $\psi(t) = at + o(t)$, $p_\psi(t) = bt + o(t)$ is plug in the equations to determine the coefficients. From the equations, we observe that the contacts with Σ differ in the case $\gamma_- = 0$ from the case $\gamma_- \neq 0$ that we discuss separately.

First of all, we consider the case $\gamma_- = 0$; $p_\theta = 0$, $\psi = 0$ is an admissible singular direction (with zero control) which can be slow if $(\gamma_+ - \Gamma) > 0$ or fast if $(\gamma_+ - \Gamma) < 0$. In the first case, there is no admissible extremal through Σ while it is possible if $\gamma_+ - \Gamma < 0$. If we compute the different orders, we have that ψ is of order t , p_ψ is of order t^2 while p_ρ has to be non zero if $p_\theta = 0$. If we consider extremals with $p_\theta \neq 0$, we can conclude with the orders alone. Indeed the Hamiltonian is $H_r = \varepsilon$, $\varepsilon = 0, 1$ and in both cases, we have:

$$-p_\rho\rho(\gamma_+ - \Gamma)\psi^2 - p_\psi\psi(\gamma_+ - \Gamma) + \sqrt{p_\psi^2 + p_\theta^2\psi^2} = 0.$$

The conclusion using orders is then straightforward. For instance, if ψ and p_ψ are of order one, this gives $p_\psi = p_\theta\psi = 0$ which is impossible. The other cases are similar.

In the case $\gamma_- \neq 0$, the analysis is more intricate and we must analyze the equations. We introduce the Hamiltonians:

$$H_1 = -p_\theta\psi, \quad H_2 = p_\psi.$$

Differentiating H_1 and H_2 with respect to t , one gets:

$$\begin{aligned}\dot{H}_1 &= \{H_1, H_0\} + v_2\{H_1, H_2\} \\ \dot{H}_2 &= \{H_2, H_0\} + v_1\{H_2, H_1\}\end{aligned}$$

and at a point of Σ , we obtain the relations:

$$\dot{H}_1 = -p_\theta(\gamma_- - v_2), \quad \dot{H}_2 = \gamma_- p_\rho - v_1 p_\theta.$$

In order to analyze the singularity, we use a polar blowing up:

$$H_1 = r \cos \alpha, \quad H_2 = r \sin \alpha,$$

and we get:

$$\begin{aligned}\dot{r} &= \gamma_- \left[-\frac{p_\theta \cos \alpha}{\rho} + p_\rho \sin \alpha \right] \\ \dot{\alpha} &= \frac{1}{r} \left[\gamma_- p_\rho \cos \alpha + \frac{p_\theta \gamma_- \sin \alpha}{\rho} - p_\theta \right].\end{aligned}$$

Hence, the extremals crossing Σ are given by solving $\dot{\alpha} = 0$, while the sign of \dot{r} is given by the first equation above.

Depending upon the parameters and the initial conditions on (p_ρ, ρ) , the equation $\dot{\alpha} = 0$ can have at most two distinct solutions on $(0, 2\pi)$, while in the case $p_\theta = 0$, we get an ordinary switching point for the single-input system. The assertion 2 is proved. \square

3.3 Geometric analysis and numerical solution

We first analyze the integrable case $\gamma_- = 0$. We only present a summary of the result of [4] in order to be generalized to the case $\gamma_- \neq 0$.

3.3.1 The case $\gamma_- = 0$

The system (7) is associated to a system on the two-sphere of revolution of the form:

$$\dot{q} = G_0(q) + \sum_{i=1}^2 u_i G_i(q).$$

It defines a Zermelo navigation problem on the two-sphere of revolution where the drift term G_0 represents the current:

$$G_0 = \frac{\sin(2\phi)}{2} (\gamma_+ - \Gamma) \frac{\partial}{\partial \phi}, \quad (11)$$

and $G_1 = \frac{\partial}{\partial \phi}$, $G_2 = -\cot \phi \frac{\partial}{\partial \theta}$ form a frame for the metric $g = d\phi^2 + \tan^2 \phi d\theta^2$ which is singular at the equator $\phi = \pi/2$. The drift can be compensated by a feedback with $|u| < 1$ if $|\gamma_+ - \Gamma| < 2$. This leads to the following discussion.

Case $|\gamma_+ - \Gamma| < 2$: In this case, the system reduced to the two-sphere defines a Finsler geometric for which the extremals are a deformation of the extremals of $g = d\phi^2 + \tan^2 \phi d\theta^2$. The main problem properties are described in the next proposition.

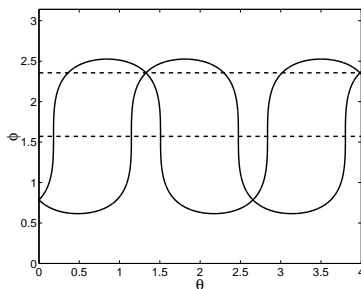


Figure 10: Extremal trajectories for $\Gamma = 2.5$, $\gamma_+ = 2$ and $\gamma_- = 0$. Other parameters are taken to be $p_\phi(0) = -1$ and 2.33 , $\phi(0) = \pi/4$, $p_\rho = 1$ and $p_\theta = 2$. Dashed lines represent the equator and the antipodal parallel located at $\phi = 3\pi/4$.

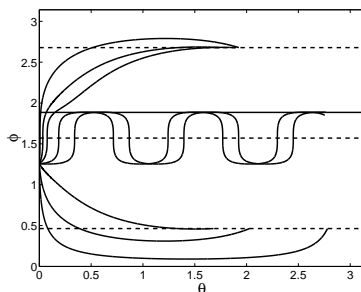


Figure 11: Extremal trajectories for $\Gamma = 4.5$, $\gamma_+ = 2$ and $\gamma_- = 0$. Dashed lines represent the equator and the locus of the fixed points of the dynamics. The solid line corresponds to the antipodal parallel. Numerical values of the parameters are taken to be $\phi(0) = 2\pi/5$, $p_\theta = 8$ and $p_\rho(0) = 0.25$. The different initial values of p_ϕ are -50 , -10 , 0 , 2.637 , 3 , 5 , 10 and 50 .

Proposition 3. *If for fixed (p_r, p_θ) , the level set of $H_r = \varepsilon$ ($\varepsilon = 0, 1$) is compact without singular point and has a central symmetry with respect to $(\phi = \pi/2, p_\phi = 0)$ then it contains a periodic trajectory (ϕ, p_ϕ) of period T and if $p_\phi^\pm(0)$ are distinct, we have two distinct extremal curves $q^+(t)$, $q^-(t)$ starting from the same point and intersecting with the same length $T/2$ at a point such that $\phi(T/2) = \pi - \phi(0)$ (see Fig. 10).*

Case $|\gamma_+ - \Gamma| > 2$: We have two types of extremals characterized by their projection on the two-sphere: those occurring in a band near the equator and described by proposition 3 and those crossing a band near $\phi = \pi/4$ and with asymptotic properties of proposition 4:

Proposition 4. *If $|\Gamma - \gamma_+| \geq 2$ then we have extremal trajectories such that $\phi \rightarrow 0$, $|p_\phi| \rightarrow +\infty$ when $t \rightarrow +\infty$ while $\dot{\theta} \rightarrow 0$.*

Both behaviors are represented on Fig. 11.

3.3.2 The case $\gamma_- \neq 0$

We present numerical results about the behavior of extremal solutions of order 0 and conjugate point analysis.

Extremal trajectories:

We begin by analyzing the structure of extremal trajectories. The description is based on a direct integration of the system (8). We observe two different asymptotic behaviors corresponding to stationary points of the dynamics which are described by the following results.

Proposition 5. *In the case denoted (a) where $|p_\phi(t)| \rightarrow +\infty$ when $t \rightarrow +\infty$, the asymptotic stationary points $(\rho_f, \phi_f, \theta_f)$ of the dynamics are given by $\rho_f = |\gamma_-| \sqrt{1 + \Gamma^2} / (1 + \gamma_+ \Gamma)$ and $\phi_f = \arctan(1/\Gamma)$ if $\gamma_- > 0$ or $\phi_f = \pi - \arctan(1/\Gamma)$ if $\gamma_- < 0$.*

Proof. We assume that $|p_\phi(t)| \rightarrow +\infty$ as $t \rightarrow +\infty$ and that $\cot(\phi)$ remains finite in this limit. One deduces from the system (8) that (ρ_f, ϕ_f) satisfy the following equations:

$$\begin{aligned} \gamma_- \cos \phi_f &= \rho_f (\gamma_+ \cos^2 \phi_f + \Gamma \sin^2 \phi_f) \\ \frac{\gamma_- \sin \phi_f}{\rho_f} &= (\gamma_+ - \Gamma) \cos \phi_f \sin \phi_f + \varepsilon, \end{aligned}$$

where $\varepsilon = \pm 1$ according to the sign of p_ϕ . The quotient of the two equations leads to

$$(\gamma_+ - \Gamma) \cos \phi_f \sin \phi_f + \varepsilon = \tan \phi_f (\gamma_+ \cos^2 \phi_f + \Gamma \sin^2 \phi_f)$$

which simplifies into

$$\tan \phi_f = \frac{\varepsilon}{\Gamma}.$$

Using the fact that $\phi_f \in]0, \pi[$ and $\gamma_- \cos \phi_f \geq 0$, one arrives to $\phi_f = \arctan(1/\Gamma)$ if $\gamma_- > 0$ and $\phi_f = \pi - \arctan(1/\Gamma)$ if $\gamma_- < 0$. From the equation

$$\gamma_- \cos \phi_f = \rho_f (\gamma_+ \cos^2 \phi_f + \Gamma \sin^2 \phi_f),$$

one finally obtains that

$$\rho_f = \frac{\gamma_- \sqrt{1 + \Gamma^2}}{1 + \gamma_+ \Gamma}.$$

□

Proposition 6. *In the case denoted (b) where $\lim_{t \rightarrow +\infty} \phi(t) = 0$ or π , the asymptotic limit of the dynamics is characterized by $\rho_f = |\gamma_-|/\gamma_+$ and $\phi_f = 0$ if $\gamma_- > 0$ or $\phi_f = \pi$ if $\gamma_- < 0$.*

Proof. Using the relation

$$\gamma_- \cos \phi_f = \rho_f (\gamma_+ \cos^2 \phi_f + \Gamma \sin^2 \phi_f),$$

one deduces that $\gamma_- \cos \phi_f \geq 0$ and that $\rho_f = |\gamma_-|/\gamma_+$ if $\phi_f = 0$ or π . □

We have numerically checked that if $|\Gamma - \gamma_+| > 2$ then only the case (a) is encountered whereas if $|\Gamma - \gamma_+| < 2$, the extremals are described by cases (a) and (b). One particularity of the case (a) is the fact that the limit of the dynamics only depends on Γ and on the sign of γ_- and not on $\phi(0)$ or γ_+ . The structure of the extremals is also simple in case (b) since the limit of ϕ is 0 or π independently of the values of Γ , γ_+ or γ_- . The different behaviors of the extremals are illustrated in Fig. 12 for the case $|\Gamma - \gamma_+| > 2$ and in Fig. 14 for the case $|\Gamma - \gamma_+| < 2$. The corresponding optimal control fields v_1 and v_2 are represented in Fig. 13 for the case (a) and in Fig 15 for the case (b). In Fig. 13, note that the control v_1 tends to 0 whereas v_2 is close to -1 for t sufficiently large. This is due to the fact that $|p_\phi| \rightarrow +\infty$ when $t \rightarrow +\infty$ and can be easily checked from the definition of v_1 and v_2 . We observe a similar behavior for the case (b) in Fig. 15. The control field v_1 acquires here a bang-bang structure which is related to the unbounded and oscillatory behavior of $p_\phi(t)$ (see Fig. 15).

Conjugate points:

The Cotcot code is used to evaluate the conjugate points. This occurs only in case (b) and the numerical simulations give that the first conjugate points appear before an uniform number of oscillations of the ϕ variable. This phenomenon is represented on Fig. 16. Cutting the trajectory at the first conjugate point avoids such a behavior. Note that due to the symmetry of revolution, the global optimality is lost for $\theta \leq \pi$.

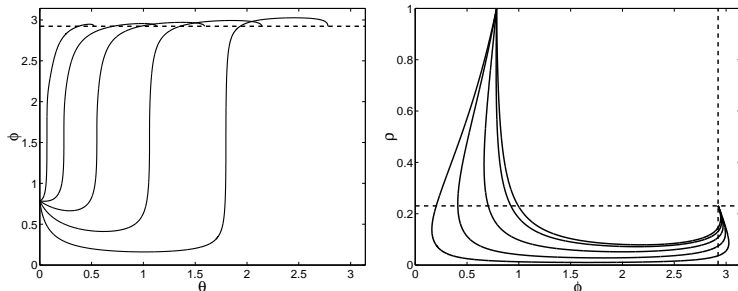


Figure 12: Extremal trajectories for $\Gamma = 4.5$, $\gamma_+ = 2$ and $\gamma_- = -0.5$. The equations of the dashed lines are $\phi = \pi - \arctan(1/\Gamma)$ and $\rho = |\gamma_-| \sqrt{1 + \Gamma^2} / (1 + \gamma_+ \Gamma)$ (see the text). Numerical values of the parameters are taken to be $\phi(0) = \pi/4$, $p_\theta = 2$, $p_\rho(0) = 0.1$ and $\rho(0) = 1$. $p_\phi(0)$ is successively equal to -10, -2.5, 0, 2.5 and 10 for the different extremals.

4 Physical conclusions

We give some qualitative conclusions on the time-optimal control of two-level dissipative systems. The discussion concerns the role of dissipation which can be beneficial or not for the dynamics and the robustness with respect to dissipative parameters of the optimal control.

The dissipation effect is well summarized by Fig. 2. In this case $\Gamma > \gamma_+$ and one sees that as long as the purity of the state decreases (for $0 \leq z \leq 1$), it is advantageous to use a control field, the dissipation being undesirable. On

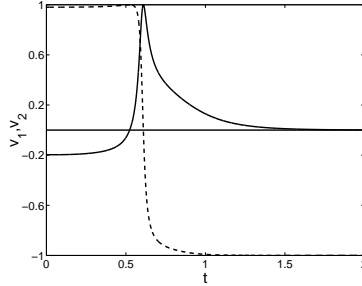


Figure 13: Plot of the optimal control fields v_1 (solid line) and v_2 (dashed line) as a function of time t for the extremal trajectory of Fig. 12 with $p_\phi(0) = 5$. The equation of the horizontal solid line is $v = 0$.

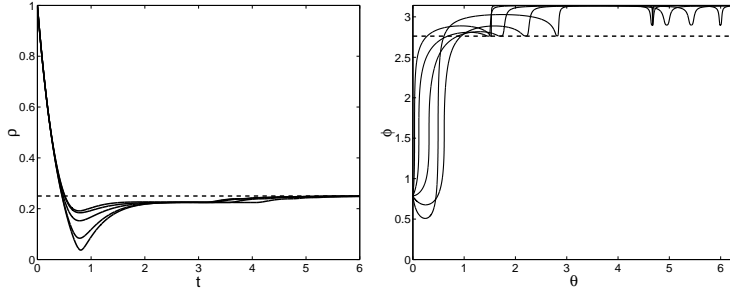


Figure 14: Same as Fig. 12 but for $\Gamma = 2.5$. The equation of the dashed line is $\rho = |\gamma_-|/\gamma_+$.

the contrary, when the purity starts increasing (for $-\gamma_-/\gamma_+ \leq z \leq 0$) then the dissipation alone becomes more efficient and its role positive. The quickest way to accelerate the purification of the state consists in letting the dissipation acts. This constitutes a non-intuitive physical conclusion which, however, crucially depends on the respective values of Γ and γ_+ . For instance, if $\gamma_+ > \Gamma$ then all the preceding conclusions are modified.

The robustness of the optimal control with respect to dissipative parameters is illustrated by the double-input control. We give different examples. If $\gamma_- = 0$ then the integrability of the Hamiltonian and the geometrical properties of the extremals are preserved when $|\Gamma - \gamma_+| < 2$. If $\gamma_- \neq 0$ then the asymptotic behavior of the extremals slightly depends on the parameters Γ , γ_+ and γ_- (see Propositions 5 and 6). Fig. 13 and 15 show that the extremal control fields have also asymptotic behaviors independent of the dissipation. In case (a), the control fields tend to a constant whereas a bang-bang structure appears in case (b). This conclusion could be interesting for practical applications where robustness with respect to physical parameters and simple control fields are needed. In addition, due to the simple structure of the time-optimal synthesis, shooting techniques will be particularly efficient to determine the control fields especially in case (a).

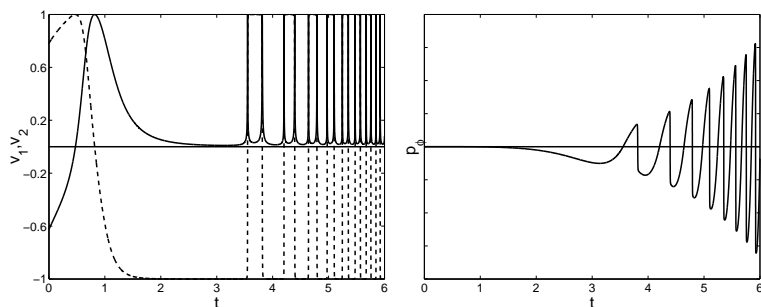


Figure 15: (top) Same as Fig. 13 but for the extremal of Fig. 14 with $p_\phi(0) = 2.5$. (bottom) Evolution of p_ϕ for the same extremal as a function of t .

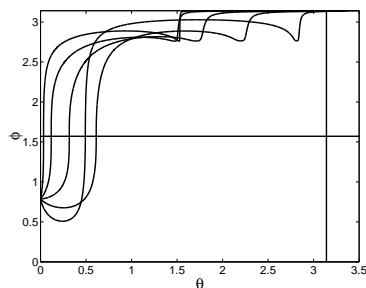


Figure 16: Plot of the extremals of Fig. 14 up to the first conjugate point. The coordinates θ of the conjugate points are respectively 3.149, 3.116, 3.332, 3.386 and 3.535 for $p_\phi(0)$ equal to -10, -2.5, 0, 2.5 and 10. The equations of the horizontal and vertical solid lines are respectively $\phi = \pi/2$ and $\theta = \pi$.

Acknowledgment

We acknowledge support from the Agence Nationale de la recherche (ANR Co-Moc).

References

- [1] C. ALTAFINI, *Controllability properties for finite dimensional quantum Markovian master equations*, J. Math. Phys. **44**, 2357 (2002).
- [2] B. BONNARD, J.-B. CAILLAU AND E. TRÉLAT, *Second-order optimality conditions in the smooth case and applications in optimal control*, ESAIM : COCV **13**, no. 2, 207-236 (2007)
- [3] B. BONNARD AND M. CHYBA, *Singular trajectories and their role in control theory*, Math. and Applications 40, Springer-Verlag, Berlin (2003)
- [4] B. BONNARD AND D. SUGNY, *Optimal control of dissipative two-level quantum systems*, submitted (2008), SIAM J. Control Optim.

- [5] B. BONNARD AND E. TRÉLAT, *Une approche géométrique du control optimal de l'arc atmosphérique de la navette spatiale*, ESAIM : COCV **7**, 179-222 (2002).
- [6] U. BOSCAIN, G. CHARLOT, J.-P. GAUTHIER, S. GUÉRIN AND H. R. JAUSLIN, *Optimal control in laser-induced population transfer for two- and three-level quantum systems*, J. Math. Phys. **43**, no. 5, 2107 (2002).
- [7] U. BOSCAIN AND B. PICCOLI, *Optimal syntheses for control systems on 2-D manifolds*, Springer-Verlag, Berlin (2003).
- [8] U. BOSCAIN AND Y. CHITOUR, *On the minimum time problem for driftless left-invariant control systems on $SO(3)$* , Comm. Pure Appl. Anal., **1**, no. 3, 128 (2002).
- [9] V. GORINI, A. KOSSAKOWSKI AND E. C. G. SUDARSHAN, *Completely positive dynamical semigroups of N -level systems*, J. Math. Phys., **17**, 821 (1976).
- [10] G. LINDBLAD, *On the generators of quantum dynamical semi-groups*, Comm. Math. Phys., **48**, 119 (1976).
- [11] H. SCHÄTTLER, *The local structure of time-optimal trajectories in dimension three under generic conditions*, SIAM J. Control Optim., **26**, no. 5, 1145-1162, (1987).
- [12] S. G. SCHIRMER AND A. I. SOLOMON, *Constraints on relaxation rates for N -level quantum systems*, Phys. Rev. A, **70**, 022107 (2004).
- [13] D. SUGNY, C. KONTZ AND H. R. JAUSLIN, *Time-optimal control of a two-level dissipative quantum system*, Phys. Rev. A, **76**, 023419 (2007).
- [14] H. J. SUSSMANN, *Regular synthesis for time-optimal control of single-input real analytic system in the plane: the general real analytic case*, SIAM J. Control Optim., **26**, no. 4, 899-918, (1988).